Spin–Lattice Relaxation in the 6H Polytype of Silicon Carbide

J. Stephen Hartman,* Arjun Narayanan, and YouXiang Wang

Contribution from the Department of Chemistry, Brock University, St. Catharines, Ontario L2S 3A1, Canada

Received September 13, 1993®

Abstract: ^{13}C and ^{29}Si spin–lattice relaxation in nitrogen-doped 6H-polytype silicon carbide is highly site-dependent. Not only do carbon sites relax much more rapidly than the corresponding silicon sites, but also there are unprecedented differences in relaxation efficiency among the different carbon, and among the different silicon, sites, that can be related to much higher unpaired electron density in the conduction band at the higher-symmetry (types A and B) sites than at the lowest-symmetry (type C) site. In contrast, all sites relax at equivalent rates in most other 6H silicon carbide samples, including both commercial abrasive grade material with high levels of impurities and high-purity aluminum-doped and undoped samples. The nature of the relaxation process differs as well, from stretched exponential in lower-purity to exponential in high-purity samples.

Introduction

Silicon carbide, a diamond-like network solid, has long been of interest because of its unique array of polytypes (forms with different layer stacking sequences), over 200 polytypes having been reported.[1] Ever since its discovery a century ago it has been important as an abrasive,[1] and recently it has attracted attention because of its great potential as a high-tech ceramic material[2] and as a high-band-gap semiconductor.[3,4] In our initial reports of the ^{29}Si and ^{13}C magic angle spinning NMR spectra of silicon carbide polytypes,[5,6] we noted the distinctive three-peak ^{29}Si and ^{13}C spectra of the 6H polytype, arising from the three nonequivalent silicon sites and from the three nonequivalent carbon sites, each of which is isostructural to one of the silicon sites. Further, different local regions of the same abrasive-grade silicon carbide sample can show very different spin–lattice relaxation efficiencies, allowing small fast-relaxing regions to contribute disproportionately to the spectrum. Others too have observed extremely inefficient relaxation, as well as an efficiently relaxing component, in 6H-polytype samples.[7] We also found evidence of great variability in spin–lattice relaxation efficiency among different samples, consistent with early low-temperature electron nuclear double resonance studies.[8]

We[9,10] and others[11] have further explored the NMR of silicon carbide polytypes. On the basis of single-crystal work, we have assigned the equal-intensity peaks of the 6H polytype to the individual lattice environments. The lowest-symmetry type C site[5,6] is assigned to the highest-frequency resonance in the ^{13}C spectrum, but to the middle resonance in the ^{29}Si spectrum.[9]

In the last decade, high resolution magic angle spinning NMR has become an important characterization method for a wide range of new inorganic materials.[12] It has unique capabilities for the characterization of heterogeneous materials.[13] MAS NMR has been useful in characterizing silicon carbide prepared by chemical vapor deposition, reaction of preceramic polymers, and other methods.[14] However the only available NMR nuclei in silicon carbide are the dilute spin-$^1/_2$ nuclei ^{29}Si and ^{13}C, and there is no effective intrinsic spin–lattice relaxation mechanism in dilute spin-$^1/_2$ rigid solids.[15] Hence the drawbacks of inefficient spin–lattice relaxation can be severe. Spin–lattice relaxation is driven by paramagnetic impurities in such systems, and can be very different in different local regions of a heterogeneous material,[16] so that NMR spectra of such a system can be misleading. Very inefficient spin-lattice relaxation can lead to the NMR signals of high-purity components being anomalously small or missed entirely. Our investigations of this limitation to quantitative NMR in synthetic[17] and natural[18] silicate minerals have been extended to the present study of spin–lattice relaxation

® Abstract published in *Advance ACS Abstracts,* March 15, 1994.

(1) *Gmelin Handbook of Inorganic Chemistry*, 8th ed.; Springer-Verlag: Berlin/Heidelberg/New York; Suppl. Vol. B2, Si-Silicon, "Properties of Crystalline Silicon Carbide", 1984; Suppl. Vol. B3, Si-Silicon, "System Si–C", 1986.

(2) (a) McColm, I. J.; Clark, N. J. *Forming, Shaping, and Working of High-Performance Ceramics*; Blackie: Glasgow and London, 1988. (b) Mackenzie, J. D.; Ulrich, D. R. *Ultrastructure Processing of Advanced Ceramics*; Wiley-Interscience: New York, 1988. (c) Zeigler, J. M.; Fearon, F. W. G., Eds. *Silicon-Based Polymer Science. A Comprehensive Resource*; Advances in Chemistry Series, No. 224; American Chemical Society: Washington, DC, 1990; especially Chapters 31, 32, and 34.

(3) Davis, R. F.; Glass, J. T. *Adv. Solid State Chem.* **1991**, *2*, 1.

(4) Ivanov, P. A.; Chelnokov, V. E. *Semicond. Sci. Technol.* **1992**, *7*, 863.

(5) Finlay, G. R.; Hartman, J. S.; Richardson, M. F.; Williams, B. L. *J. Chem. Soc., Chem. Commun.* **1985**, 159.

(6) Hartman, J. S.; Richardson, M. F.; Guo, D.; Winsborrow, B. G. *J. Am. Chem. Soc.* **1987**, *109*, 6059.

(7) Mooney, J. R. In *Analytical NMR*; Field, L. D., Sternhell, S., Eds.; John Wiley and Sons, Chichester, 1989; Chapter 3, Section 3.3.

(8) (a) Hardeman, G. E. G. *J. Phys. Chem. Solids* **1963**, *24*, 1223. (b) Alexander, M. N. *Phys. Rev.* **1968**, *172*, 331.

(9) Richardson, M. F.; Hartman, J. S.; Guo, D.; Winsborrow, B. G. *Chem. Mater.* **1992**, *4*, 318.

(10) Guo, D.; Hartman, J. S.; Richardson, M. F. *Can. J. Chem.* **1992**, *70*, 700.

(11) Guth, J. R.; Petuskey, W. T. *J. Phys. Chem.* **1987**, *91*, 5361. Apperley, D. C.; Harris, R. K.; Marshall, G. L.; Thompson, D. P. *J. Am. Ceram. Soc.* **1991**, *74*, 777. Wagner, G. W.; Na, B. K.; Vannice, M. A. *J. Phys. Chem.* **1989**, *93*, 5061.

(12) Engelhardt, G.; Michel, D. *High-Resolution Solid-State NMR of Silicates and Zeolites*; John Wiley & Sons: Chichester, 1987. Hatfield, G. R.; Carduner, K. R. *J. Mater. Sci.* **1989**, *24*, 4209. Eckert, H. *Ber. Bunsenges. Phys. Chem.* **1990**, *94*, 1062. Eckert, H. *Prog. NMR Spectrosc.* **1992**, *24*, 159.

(13) Blumich, B. *Adv. Mater.* **1991**, *3*, 237.

(14) Turner, G. L.; Kirkpatrick, R. J.; Risbud, S. H.; Oldfield, E. *Am Ceram. Soc. Bull.* **1987**, *66*, 656. Lipowitz, J.; Freeman, H. A.; Chen, R. T.; Prack, E. R. *Adv. Ceram. Mater.* **1987**, *2*, 121. Taki, T.; Inui, M.; Okamura, K.; Sato, M. *J. Mater. Sci. Lett.* **1989**, *8*, 918. Carduner, K. R.; Shinozaki, S. S.; Rokosz, M. J.; Peters, C. R.; Whalen, T. J. *J. Am. Ceram. Soc.* **1990**, *73*, 2281. Zhang, Z.-F.; Babonneau, F.; Laine, R. M.; Mu, Y.; Harrod, J. F.; Rahn, J. A. *J. Am. Ceram. Soc.* **1991**, *74*, 670. Schmidt, W. R.; Interrante, L. V.; Doremus, R. H.; Trout, T. K.; Marchetti, P. S.; Maciel, G. E. *Chem. Mater.* **1991**, *3*, 257. Burns, G. T.; Taylor, R. B.; Xu, Y.; Zangvil, A.; Zank, G. A. *Chem. Mater.* **1992**, *4*, 1313. Laine, R. M.; Babonneau, F. *Chem Mater.* **1993**, *5*, 260. Tougne, P.; Hommel, H.; Legrand, A. P.; Herlin, N.; Luce, M.; Cauchetier, M. *Diamond Relat. Mater.* **1993**, *2*, 486. Dando, N. R.; Perrotta, A. J.; Strohmann, C.; Stewart, R. M.; Seyferth, D. *Chem. Mater.* **1993**, *5*, 1624.

(15) (a) Abragam, A. *The Principles of Nuclear Magnetism*; Clarendon: Oxford, 1961; Chapters V and IX. (b) Abragam, A.; Goldman, M. *Nuclear Magnetism: Order and Disorder*; Clarendon: Oxford, 1982; Chapter VI.

(16) (a) Axelson, D. E. *Solid State Nuclear Magnetic Resonance of Fossil Fuels: An Experimental Approach*; Multiscience Publications Limited: Canadian Government Publishing Centre, Supply and Services Canada: Ottawa, Ontario, Canada, 1985; Chapter 3. (b) Wind, R. A.; Maciel, G. E.; Botto, R. E. In *Magnetic Resonance of Carbonaceous Solids*; Botto, R. E., Sanada, Y., Eds.; Advances in Chemistry Series, No. 229; American Chemical Society: Washington, DC, 1993; Chapter 1.

0002-7863/94/1516-4019$04.50/0 © 1994 American Chemical Society

in silicon carbide. Highly inefficient spin–lattice relaxation in silicon carbide is compensated by the very high concentration (80 M) of both silicon and carbon, which allows strong NMR signals to be obtained in a single scan. This, plus the total of six very similar but not identical sites to study (three ^{29}Si and three ^{13}C), makes the 6H polytype of silicon carbide an ideal model system for the study of spin–lattice relaxation in dilute-spin rigid solids. Relaxation behavior of two different dilute spin-$^1/_2$ nuclei in isomorphous environments in the same sample can be compared.

Experimental Section

Materials. Nitrogen- and aluminum-doped semiconductor-grade 6H silicon carbide samples were purchased from Cree Research, Inc., Durham, NC. Dopant concentrations were determined at Cree Research by the capacitance-voltage technique using a double column MDC Hg probe and a Keithley 590 C-V analyzer. However the determinations were done on nearby slices of large single crystals, rather than the slices obtained by us, so some discrepancy in nitrogen content is possible. Other impurities in these samples are reported to be at or below the 2 ppm level.

Lely furnace 6H silicon carbide samples, undoped, doped with nitrogen at high and low levels, and doped with known levels of boron, aluminum, and nitrogen as determined by secondary ion mass spectrometry, were provided by Prof. Robert F. Davis, North Carolina State University, Raleigh, NC. The boron/aluminum/nitrogen-doped sample is homogeneous down to 10 μm, by back scattering electron analysis using an electron microprobe.[19] Further silicon carbide samples include the following: (i) the National Bureau of Standards Standard Reference Material 112b, 97.37% silicon carbide,[20] reported to contain a mixture of polytypes including 6H,[21] and very inhomogeneous by back scattering electron analysis[19] (the homogeneous silicon carbide phase is accompanied by a separate material with two metals-rich phases, one rich in Fe, Ti, Ni, Cu, and Si and the second rich in Fe, Ni, Si, Al, and Mg); (ii) a commercial Acheson furnace abrasive grade 6H silicon carbide sample (BGW43) from General Abrasive, Niagara Falls, Ontario, homogeneous by electron microprobe analysis; (iii) a 6H sample (SiC008) from the personal collection of the late Dr. Gordon R. Finlay of Brock University; and (iv) a 6H single crystal platelet sample from American Matrix Inc., Knoxville, TN.

Nitrogen-doped samples are typically green; our aluminum-doped sample is gray, while the undoped sample has the appearance of clear, colorless window glass. Abrasive grade and other less-pure samples are typically dull gray to black. All samples become dull gray when powdered in a tungsten carbide ball mill; we cannot exclude contamination by tungsten carbide in our powder samples because 6H silicon carbide is such an excellent abrasive, but any relaxation effects of such contamination are apparently negligible.

NMR Spectra. ^{29}Si and ^{13}C magic angle spinning NMR spectra were obtained on Bruker AC-200 (4.7 T) and AM-500 (11.7 T) multinuclear Fourier transform NMR instruments. On the 4.7 T instrument, home-built magic angle spinning probes of the Andrew–Beams type[22] and Delrin rotors were used, and powdered samples were spun at 3.0–3.6 kHz at an angle of 54°44′ to the magnetic field. Spectra were obtained with 8K data points, frequencies of 39.76 MHz (^{29}Si) and 50.3 MHz (^{13}C), and spectral widths between 10 and 50 kHz. The 90° pulse was close to 25 μs for both nuclei. On the 11.7 T instrument, a Doty high-speed magic angle spinning probe was used, with 5 mm rotors and spinning speeds of up to 8 kHz. Spectra were obtained with 8K data points, a frequency of 99.3 MHz (^{29}Si) and 125.7 MHz (^{13}C), and spectral widths between 30 and 50 kHz. The 90° pulse width was close to 6 μs for both nuclei. Variations in spinning speed between 1 and 8 kHz had little effect on the efficiency of spin–lattice relaxation.

The saturation recovery method was used for determination of spin–lattice relaxation behavior. A train of pulses (progressive saturation sequence) was used to saturate the nuclear magnetization, with from 10 to 50 short pulses separated by delays of the order of 10 μs (for the fastest-relaxing samples) up to 1 s (for the slowest-relaxing samples). The delays between pulses should not all be the same; typically we found that a repeating sequence of three different delay times in the ratio of 10:9:8 gave effective nulling of the magnetization. Following the train of pulses and a variable delay time τ, a 90° pulse was applied and the FID acquired. To avoid damaging capacitors in our home-built magic angle spinning probes, work at 4.7 T on fast-relaxing samples utilized a long sequence of 50 or more very short (about 1 μs) pulses, rather than a smaller number of 30° or 90° pulses.

Because of very slow relaxation and limitations on the instrument time available, only a single scan was obtained for each delay time τ whenever possible. This was possible for the higher-purity samples with sharp peaks, for both ^{29}Si and ^{13}C at 11.7 T, and also for ^{29}Si at 4.7 T, although signal-to-noise ratios were sometimes marginal. Four scans were required to obtain usable ^{13}C spectra of even the best silicon carbide samples at 4.7 T. Less pure samples with broad and poorly resolved peaks required additional scans.

The inversion recovery (180°–τ–90°) pulse sequence was also used with a few of the faster-relaxing samples. Good agreement was attained with the saturation recovery results, provided that a sufficiently long fixed delay was applied. However this method is impractical with slow-relaxing samples.[23]

Fitting Procedures and Error Analysis. The time constant T' and the exponent n, indicating the degree of stretch of the stretched exponential decay function, were obtained from four parameter least-squares fits, using (i) commercially available software (DeltaGraph Professional, DeltaPoint Inc., Monterey, CA) and (ii) the program STRETCHR, developed by Prof. A. D. Bain of McMaster University. Because two parameters rather than one must be determined, data sets of at least 15 to 20 τ values were used whenever possible. A function of the form

$$y = a - be^{-(\tau/T')^n} \quad (1)$$

was fitted to the data to estimate T' and n, using a standard nonlinear least-squares approach.[24] The parameters a and b were fitted separately in order to account for any possible effects of poor baselines as well as the possible incomplete nulling of the z-magnetization by the saturation pulse train. In most cases a and b were found to be essentially identical, as expected. In general, good fits to the stretched exponential function are obtained.

Estimates of uncertainties for the two parameters T' and n were obtained by several methods, including the method of projecting the error ellipsoids onto the parameter axes.[25] Despite the good fits to the stretched exponential function, a problem with stretched exponential curve fitting is that the values of T' and n are often correlated, with only a shallow minimum, so that there are often large errors in both. Because of this, only our best data sets give values of n that are accurate to within ±0.1 and values of T' to within ±10%. Error limits are much greater for very slowly relaxing samples in which time limitations prevented us from obtaining the full decay curve. In cases where the results are consistent with exponential relaxation, the relaxation time can be estimated with greater precision by fixing the exponent n at 1, i.e., T_1 values rather than T' (for stretched exponential) values are determined. But there are many cases where relaxation is clearly stretched exponential.

The standard deviations are indicated in the tables. The 95% confidence limits were found to be between two and three times the standard deviations[26] for both T' and n, depending on the method used. Our error analysis work on stretched exponential systems will be reported in detail elsewhere. It should be noted that, even when relaxation is known to be exponential and the signal-to-noise ratio is far better than is accessible to us in the present work, errors in T_1 values can be large.[26]

Results

(a) Nature of the Relaxation Process. As in silicate minerals,[17,18] spin–lattice relaxation does not always follow the

(17) (a) Hartman, J. S.; Sliwinski., D. R.; Cherniak, E. A. 32nd Experimental NMR Spectroscopy Conference, St. Louis, April 1991; poster P134. (b) Hartman, J. S.; Rigby, S. S.; Sliwinski, D. R. *EOS (Transactions, American Geophysical Union)* **1992**, *73*, 344. Hartman, J. S.; Narayanan, A.; Rigby, S. S.; Sliwinski, D. R.; Wang, Y.X. Eleventh International Meeting on NMR Spectroscopy, Swansea, Wales, July 1993, Poster E.8; paper in preparation.
(18) Hartman, J. S.; Sherriff, B. L. *J. Phys. Chem.* **1991**, *95*, 7575.
(19) Halden, N. M., University of Manitoba, private communication.
(20) National Bureau of Standards Certificate of Analysis.
(21) Frevel, L. K.; Petersen, D. R.; Saha, C. K. *J. Mater. Sci.* **1992**, *27*, 1913.
(22) Fyfe, C. A.; Gobbi, G. C.; Hartman, J. S.; Lenkinski, R. E.; O'Brien, J. H.; Beange, E. R.; Smith, M. A. R. *J. Magn. Reson.* **1982**, *47*, 168.
(23) Fukushima, E.; Roeder, S. B. W. *Experimental Pulse NMR. A Nuts and Bolts Approach*; Addison-Wesley: Reading, MA, 1981; Chapter III.
(24) Press, W. H.; Teukolsky, S. A.; Vetterling, W. H.; Flannery, B. P. *Numerical Recipes in C: The Art of Scientific Computing*, 2nd ed.; Cambridge University Press: Cambridge, 1992; Chapter 15.
(25) Seber, G. A. F.; Wild, C. J. *Nonlinear Regression*; Wiley Series in Probability and Mathematical Statistics; John Wiley: New York, 1989.
(26) Bain, A. D. *J. Magn. Reson.* **1990**, *89*, 153.

Table 1. Spin–Lattice Relaxation Parameters for Undoped and Al-Doped 6H SiC

	^{29}Si				^{13}C			
	peak (ppm)	T_1[a] (s)	n	no. of points[b]	peak (ppm)	T_1[a] (s)	n	no. of points[b]
				(a) 11.7 T				
undoped	−14	18800 ± 5%	1.0 ± 0.1	9	23	27000 ± 45%	1.0 ± 0.5	8
	−21	19700 ± 8%	1.2 ± 0.1	9	20	18000 ± 17%	1.0	8
	−25	18500 ± 4%	1.0 ± 0.1	9	15	50000 ± 50%	1.5 ± 0.3	8
Al doped[c]	−14	9300 ± 7%	0.9 ± 0.1	17	23	12500 ± 18%	1.2 ± 0.2	20
	−21	8700 ± 6%	0.9 ± 0.1	17	20	11900 ± 21%	1.3 ± 0.3	22
	−25	8100 ± 4%	0.9 ± 0.1	17	15	10800 ± 21%	1.0 ± 0.4	23
				(b) 4.7 T				
undoped	−14	16000 ± 8%	1.1 ± 0.1	10	23	19800 ± 4%	0.9 ± 0.2	6
	−21	17500 ± 10%	1.4 ± 0.1	10	20	16500 ± 3%	0.9 ± 0.1	6
	−25	14200 ± 7%	1.2 ± 0.1	10	15	21400 ± 26%	0.9	6
Al doped[c]	−14	11000 ± 10%	1.0 ± 0.1	14	23	6300 ± 25%	0.9 ± 0.4	8
	−21	10200 ± 6%	1.1 ± 0.1	16	20	7600 ± 31%	1.0 ± 0.5	8
	−25	11600 ± 18%	1.3 ± 0.2	15	15	14000 ± 66%	1.0 ± 0.5	8

[a] Calculated assuming $n = 1$. [b] Number of data points used for the least-squares fit. [c] Al concentration: 8×10^{17} atoms/cm^3.

exponential rate law

$$M_z(t) \propto \exp\left[-\frac{t}{T_1}\right] \quad (2)$$

but instead a stretched exponential expression

$$M_z(t) \propto \exp\left[-\left(\frac{t}{T'}\right)^n\right] \quad (3)$$

must be applied, where n frequently takes the value of 0.5.[18,27] The time constant T_1 refers specifically to exponential relaxation,[23] so the term T' is used when $n < 1$. Empirically determining n by curve fitting gives a value of n between 0.5 and 1 that corresponds to the "degree of stretch" of the stretched exponential, which varies in different silicon carbide samples.

(b) High-Purity Silicon Carbide: Undoped and Aluminum Doped. In the highest-purity silicon carbide samples spin–lattice relaxation is exponential, is essentially independent of magnetic field, and is extremely slow with time constants of several hours (Table 1). Figure 1 illustrates the fit of the experimental points to the exponential function and the similar relaxation behavior of all three distinct ^{29}Si sites. The ^{13}C spectra behave similarly. Because of instrument time limitations, even with a single scan it was not possible in most cases to obtain the full relaxation curve. Figure 1a does show the fit of a full curve; relaxation is essentially complete following the longest delay of 25 h. Figure 1b shows a more typical fit where the total available instrument time of about 24 h did not allow delays longer than 6 h. Not defining the curve for longer τ values limits the accuracy of the T_1 and n values of Table 1, especially for ^{13}C and at 4.7 T where signal strength is less. Obtaining more than a single scan at each τ value is not normally an option for such slow-relaxing systems.

(c) High-Purity Silicon Carbide: Nitrogen Doped. Spin–lattice relaxation is exponential and essentially independent of magnetic field, but it is highly dependent on both the nitrogen concentration and the individual site, with great differences even between individual sites of the same nucleus in the same sample (Table 2). Figure 2 shows a stacked plot of ^{13}C saturation recovery spectra for a sample with an intermediate level of nitrogen (4.5×10^{17} atoms/cm^3). At intermediate τ values two of the signals have almost completely recovered their full intensity while the third has barely begun to relax. Figures 3 and 4 show the relaxation curves for typical ^{13}C and ^{29}Si spectra and illustrate the discrepancies in relaxation behavior among sites. A good fit to the data is obtained in all cases except for the slowest-relaxing carbon site at very short τ values. Here a slight excess of intensity is consistently observed. This might arise from an additional relaxation mechanism that is swamped by the more efficient relaxation in all other sites so it is detectable only at this site, or it could be an artifact of the relatively poor signal-to-noise ratio.

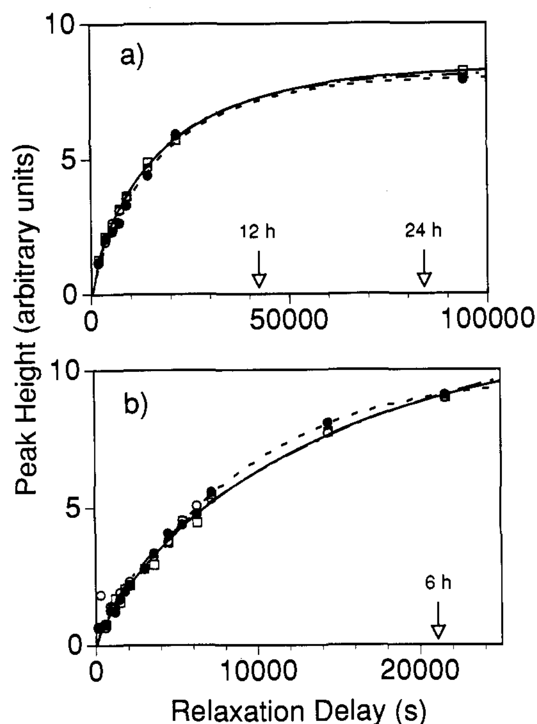

Figure 1. Plots of MAS NMR peak intensity vs saturation recovery delay time τ for the three ^{29}Si peaks of 6H silicon carbide, showing the curves obtained from a four-parameter least-squares fit: (□) −14 ppm peak; (●) −21 ppm peak; (○) −25 ppm peak. (a) "Undoped", 11.7 T; attaining equilibrium magnetization requires at least 24 h. (b) Aluminum doped, 8×10^{17} atoms/cm^3, 4.7 T.

With T_1 values differing by a factor of 20 between the low-field ^{13}C peak and the other two peaks, misleading two-peak spectra are obtained if the recovery delay is <5 min. There is a similar but less pronounced effect in the ^{29}Si spectra, with a factor of 4 between T_1 values of the two faster-relaxing sites and the slowest-relaxing site. In this case all three peaks are visible even with short recovery delays, but the center one is of misleadingly low intensity when inadequate time is allowed for its magnetization to recover. (This effect did mislead us in our initial report of silicon carbide MAS NMR.[5])

The factor of 20 between ^{13}C T_1 values for different sites in the sample, and the corresponding factor of 4 for ^{29}Si T_1 values, are maintained over the full range of nitrogen concentrations studied, as illustrated by plots of $1/T_1$ vs nitrogen dopant concentration (Figure 5). ($1/T_1$ is the first-order rate constant for spin–lattice relaxation.) The correlation is reasonably linear

(27) (a) Lowe, I. J.; Tse, D. *Phys. Rev.* **1968**, *166*, 279. (b) Rorschach, H. E., Jr. *Physica* **1964**, *30*, 38.

Table 2. Spin-Lattice Relaxation Parameters for N-Doped 6H SiC Samples

	^{29}Si				^{13}C			
[N] (atoms/cm^3)	peak (ppm)	T_1[a] (s)	n	no. of points[b]	peak (ppm)	T_1[a] (s)	n	no. of points[b]
				(a) 11.7 T				
9 × 10^{16}	−14	12300 ± 8%	1.0 ± 0.1	15	23	24800 ± 61%	1.5 ± 0.6	12
	−21	24700 ± 23%	1.0 ± 0.4	13	20	1700 ± 12%	0.8 ± 0.2	19
	−25	12500 ± 6%	1.0 ± 0.1	14	15	1800 ± 11%	0.8 ± 0.1	18
4.5 × 10^{17}	−14	3700 ± 4%	1.0 ± 0.1	19	23	4000 ± 7%	1.1 ± 0.1	20
	−21	12200 ± 12%	1.1 ± 0.2	16	20	220 ± 7%	0.7 ± 0.2	21
	−25	3200 ± 4%	1.0 ± 0.1	19	15	220 ± 6%	0.9 ± 0.2	21
1.45 × 10^{18}	−14	1340 ± 2%	1.0 ± 0.1	22	23	1400 ± 10%	1.2 ± 0.2	23
	−21	5600 ± 2%	1.0 ± 0.1	21	20	80 ± 10%	0.9 ± 0.3	26
	−25	1200 ± 3%	1.0 ± 0.1	24	15	80 ± 11%	0.6 ± 0.4	26
				(b) 4.7 T				
9 × 10^{16}	−14	14700 ± 13%	1.0 ± 0.3	17	23	18400 ± 41%	0.9	6
	−21	28900 ± 34%	0.9 ± 0.7	16	20	1700 ± 8%	0.8	18
	−25	18100 ± 26%	1.0	17	15	1900 ± 8%	0.7 ± 0.2	18
4.5 × 10^{17}	−14	4500 ± 8%	1.1 ± 0.1	19	23	4200 ± 4%	1.0 ± 0.1	23
	−21	11800 ± 12%	1.2 ± 0.2	10	20	250 ± 5%	0.9 ± 0.1	26
	−25	4500 ± 9%	1.1 ± 0.1	19	15	220 ± 3%	1.0 ± 0.1	26
1.45 × 10^{18}	−14	1400 ± 7%	1.0 ± 0.1	27	23	1500 ± 5%	0.9 ± 0.1	13
	−21	5000 ± 8%	1.0 ± 0.2	24	20	90 ± 10%	1.2 ± 0.2	16
	−25	1100 ± 6%	0.9 ± 0.1	28	15	90 ± 5%	1.0 ± 0.1	16

[a] Calculated assuming $n = 1$. [b] Number of data points used for the least-squares fit.

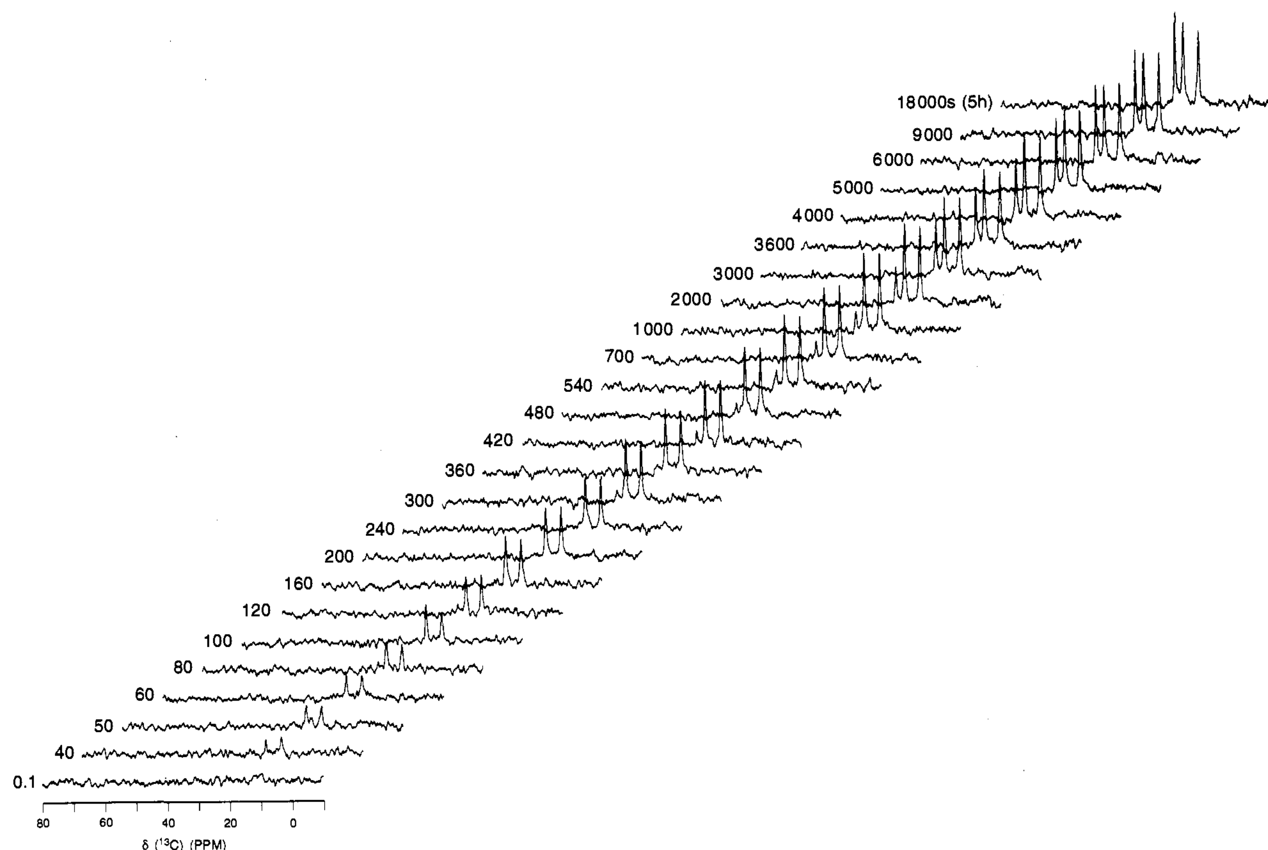

Figure 2. Stacked plot of 11.7 T ^{13}C MAS NMR spectra of nitrogen-doped (4.5 × 10^{17} atoms/cm^3) 6H silicon carbide, with saturation recovery delay times τ (s) as shown. A single scan was obtained at each τ value. At intermediate τ values only two peaks can be detected due to the much less efficient relaxation of the low-field (+23 ppm) peak.

for all sites, showing a direct relationship between nitrogen dopant concentration and relaxation efficiency.

In both the ^{29}Si and ^{13}C spectra it is the signal assigned to the type C (lowest symmetry) site[9] that relaxes the least efficiently, while the signals assigned to the types A and B sites relax equally efficiently. Further, the T_1 values of the two faster-relaxing silicon sites are the same, within experimental error, as the T_1 value of the slower-relaxing carbon site.

(d) Intermediate Purity Silicon Carbide. Table 3 gives spin-lattice relaxation data for a relatively fast-relaxing 6H silicon carbide sample, heavily doped with boron, that gives excellently-resolved NMR peaks. Relaxation is stretched exponential with $n = 0.7$ at both 4.7 and 11.7 T. ^{29}Si and ^{13}C T' values at both magnetic field strengths are all rather similar. There is however an appreciable decrease in ^{29}Si relaxation efficiency as field strength increases from 4.7 to 11.7 T, with T' values increasing by less than a factor of 2. The same effect is not observed in the ^{13}C spectra, where errors in curve fitting are larger due to a poorer signal-to-noise ratio. This sample, like the higher-purity samples of sections b and c above, gives the same peak widths regardless of the delay τ for recovery of magnetization, and this

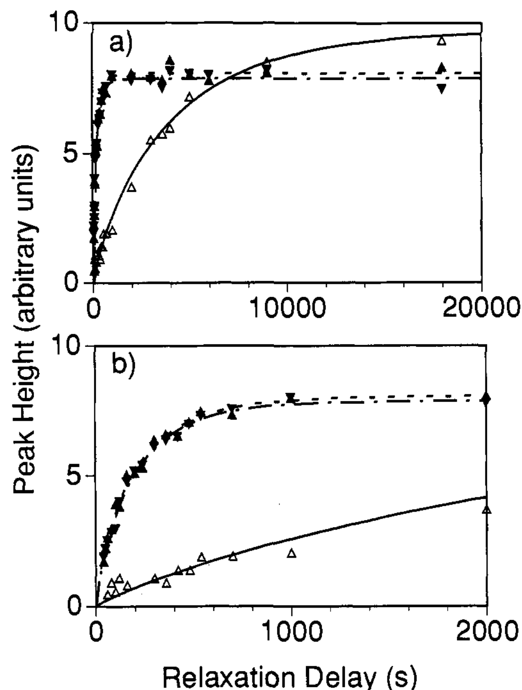

Figure 3. Plot of MAS NMR peak intensity vs saturation recovery delay time τ for the three ^{13}C peaks of a 6H silicon carbide sample doped with nitrogen at a level of 4.5×10^{17} atoms/cm^3: (△) +25 ppm peak; (▲) +20 ppm peak; (▼) +15 ppm peak. (a) The full curve; (b) the first 2000 s.

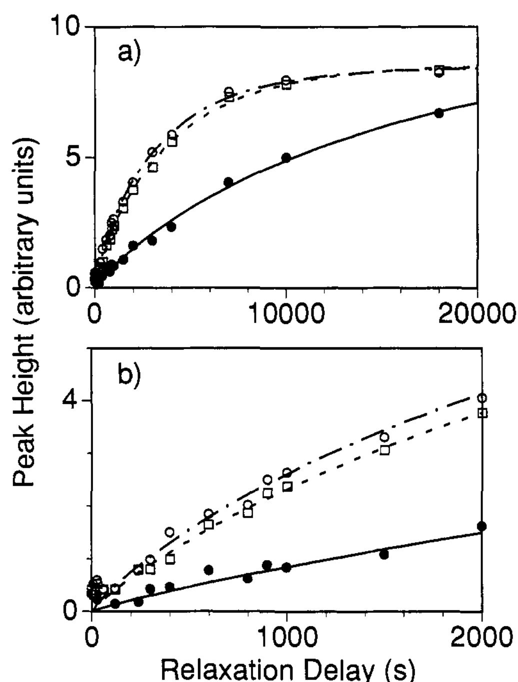

Figure 4. Plot of MAS NMR peak intensity vs saturation recovery delay time τ for the three ^{29}Si peaks of a 6H silicon carbide sample doped with nitrogen at a level of 4.5×10^{17} atoms/cm^3: (□) −14 ppm peak; (●) −21 ppm peak; (○) −25 ppm peak. (a) The full curve; (b) the first 2000 s.

indicates high sample homogeneity: there are no fast-relaxing local regions with broad NMR signals.

(e) Lower-Purity Silicon Carbide. 6H silicon carbide samples from a variety of sources give ^{29}Si spectra that are generally less well resolved that the higher-purity samples. In constrast to the semiconductor grade material, the appearance of the spectrum frequently depends on the τ value between saturation and detection. In the National Bureau of Standards 112b sample in particular, in which the three ^{29}Si peaks have unequal intensities that are consistent with an admixture of other polytypes in addition

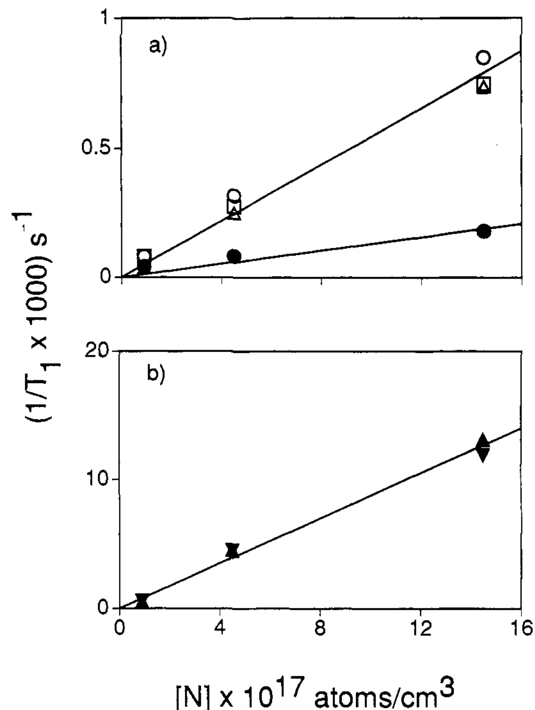

Figure 5. Plot of $1/T_1$ vs dopant concentration for nitrogen-doped 6H silicon carbide samples. (a) The intermediate and slow relaxing sites: (□) −14 ppm (^{29}Si); (○) −25 ppm (^{29}Si); (●) −21 ppm (^{29}Si); (△) +25 ppm (^{13}C). (b) The fast relaxing sites: (▲) +20 ppm (^{13}C); (▼) +15 ppm (^{13}C).

to 6H,[21] short τ values lead to broader signals, and very short τ values give only a broad blob in the silicon carbide absorption region, suggesting the presence of a very fast relaxing amorphous component (Figure 6).

This is consistent with such samples being heterogeneous. Their different local environments, which differ in relaxation efficiency, give rise to different peak resolution and sometimes to different peaks. The selection of short or long τ values allows only fast-relaxing, or both fast- and slow-relaxing, components to appear in the spectrum.[5,6] It is difficult to obtain meaningful T' and n values on such samples, since spectra obtained at different τ values will contain differing relative contributions from local regions with fast and slow relaxation characteristics. Furthermore, the broader peaks require more scans. Nevertheless, our crude ^{29}Si data (Table 4) show that stretched exponential relaxation frequently occurs. Due to limitations on instrument time we have not been able to obtain meaningful ^{13}C T' or n values for any of these samples. Our attempts at obtaining ^{13}C data do indicate that, within the same sample, ^{13}C relaxation efficiency is similar to ^{29}Si relaxation efficiency.

A cubic (β-SiC) sample is included in Table 4. It undergoes stretched exponential ^{29}Si spin–lattice relaxation ($n = 0.7$) at similar rates at both 4.7 and 11.7 T.

Discussion

(a) General. The excruciatingly long times required for relaxation in "undoped" 6H silicon carbide show conclusively that impurities do dominate the spin–lattice relaxation of all of the other samples. Our "undoped" sample gives T_1 values of about 5 h, but even this need not be an inherent limiting value, as some impurities are no doubt present in even our highest-purity samples.

A wide range of spin–lattice relaxation behaviors is encountered. The most striking difference is the exponential ($n = 1$) relaxation in the high-purity samples of Tables 1 and 2 vs the pronounced stretched-exponential ($n = 0.8$ and below) relaxation in the lower-purity samples of Tables 3 and 4: an indication of different kinetics

Table 3. Spin–Lattice Relaxation Parameters for a High-Dopant-Level 6H SiC Sample[a]

^{29}Si				^{13}C			
peak (ppm)	T' (s)	n	no. of points[b]	peak (ppm)	T'	n	no. of points[b]
(a) 11.7 T							
−14	160 ± 9%	0.65 ± 0.06	29	23	70 ± 13%	0.82 ± 0.09	25
−21	160 ± 10%	0.54 ± 0.06	29	20	80 ± 10%	0.75 ± 0.06	25
−25	160 ± 10%	0.63 ± 0.06	29	15	80 ± 12%	0.70 ± 0.06	25
(b) 4.7 T							
−14	100 ± 7%	0.71 ± 0.03	28	23	90 ± 17%	0.70 ± 0.12	23
−21	110 ± 6%	0.70 ± 0.03	30	20	100 ± 18%	0.71 ± 0.11	23
−25	120 ± 9%	0.73 ± 0.04	30	15	100 ± 20%	0.66 ± 0.12	23

[a] [B] = 1.5×10^{19} atoms/cm^3, [Al] = 1.3×10^{18} atoms/cm^3, [N] = 2.4×10^{18} atoms/cm^3. [b] Number of data points used for the least-squares fit.

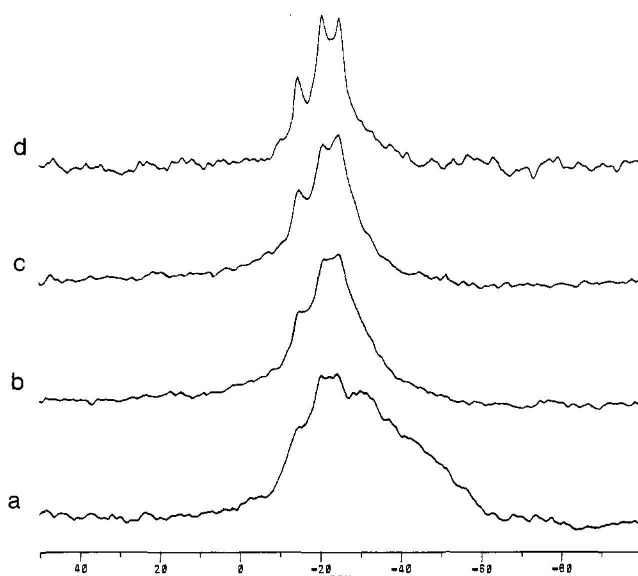

Figure 6. 4.7 T ^{29}Si saturation recovery MAS NMR spectra of the low-purity silicon carbide sample NBS 112b, showing the changed appearance of the spectrum as the recovery delay τ changes. (a) 512 scans, τ = 10 s; (b) 64 scans, τ = 100 s; (c) 32 scans, τ = 200 s; (d) 4 scans, τ = 1000 s. Short τ values bias the spectrum in favor of fast-relaxing broad components which constitute only a small fraction of the sample.

and different impurity-based mechanisms. The nature of the process clearly changes. Higher levels of fixed impurities should tend to a limiting n = 0.5 stretched exponential relaxation.[27]

Other differences are the following: (i) moderately efficient vs extremely inefficient relaxation; (ii) all sites relaxing similarly vs pronounced differences among sites; and (iii) dependence on, vs independence of, the applied magnetic field. Exponential relaxation always goes together with independence of magnetic field strength, while stretched-exponential relaxation seems to correlate with a moderate inverse dependence of relaxation efficiency on field strength, where data of sufficient accuracy are available. The high-purity nitrogen-doped samples are unique in showing pronounced differences in relaxation among different sites in the same sample.

Our slowest-relaxing samples undergo exponential relaxation. Nevertheless efficient relaxation too can be exponential. The two carbon sites in the highest-concentration nitrogen-doped sample relax faster, and with n = 1 (Table 2), than all sites of the heavily-doped sample of Table 3 (with n = 0.7), or any of the lower-purity samples that undergo stretched exponential relaxation.

(b) Origins of Stretched Exponential Relaxation. Stretched exponential processes are frequently encountered in chemical reactions and physical relaxation processes in disordered systems such as glasses.[28] Our silicon carbide samples are crystalline, but random distribution of fixed paramagnetic centers can introduce disorder. Some NMR-active atoms are nearer than others to the fixed paramagnetic centers and are more readily relaxed. "In ordered systems, all sites are the same and relax in random order, leading to an exponentially decaying signal. Paradoxically, in disordered systems the sites relax in a hierarchical order because disorder makes the sites different." [29]

Spin–lattice relaxation of spin-$^1/_2$ nuclei in liquids is normally exponential because molecular motions bring all structurally equivalent nuclei into the same averaged environment (and also permit a number of molecular-tumbling-based relaxation mechanisms that are not possible in rigid solids). In favorable circumstances, all structurally equivalent nuclei in solids can also be brought into the same relaxation environment. Often this occurs by spin diffusion: mutual spin flips of like nuclei (Chapter IX of ref 15a). Since spin diffusion is based on dipolar interactions between the exchanging spins, which drop off with distance as $1/r^6$, it is efficient with abundant nuclei such as protons and ^{19}F, but inefficient or absent with magnetically dilute nuclei such as ^{13}C and ^{29}Si.

In the absence of spin diffusion, each nucleus will be relaxed directly (through space) by the nearest paramagnetic center. Since the electron–nuclear interaction is also dipolar with a $1/r^6$ dependence, nuclei far from paramagnetic centers relax extremely slowly while those nearby relax extremely rapidly. Stretched exponential relaxation follows from this.[27] For every distance from the nearest paramagnetic center, there will be a T_1 value. It is the sum of the relaxation behavior of all of these different relaxation environments, with different distances from the nearest paramagnetic center, that inherently gives stretched-exponential relaxation. The exponent n should be 0.5 in the absence of spin diffusion,[27] as we and others have found for ^{29}Si in several silicate minerals,[17,18,30,31] although a more complex relationship is reported for paramagnetics distributed on a silica surface,[32] and spin–lattice relaxation is found to relate to the fractal dimension for paramagnetics-doped silica aerogels.[33]

This picture implies very similar relaxation behavior for ^{29}Si and ^{13}C in silicon carbide. Wherever the fixed paramagnetic centers are located, there will be equal numbers of silicon and carbon atoms nearby, and the distribution of distances to the nearest impurity should be essentially the same for both nuclei. The only difference in relaxation behavior should arise from the somewhat greater magnetic moment of ^{13}C than ^{29}Si (1.26:1), which should give somewhat more efficient relaxation for ^{13}C than ^{29}Si. Very similar ^{29}Si and ^{13}C relaxation behavior is indeed observed when stretched exponential relaxation occurs (Table 3). ^{13}C should relax slightly more efficiently than ^{29}Si, but because of the large experimental errors these small differences cannot be reliably determined.

(28) (a) Siebrand, W.; Wildman, T. A. *Acc. Chem. Res.* **1986**, *19*, 128. (b) Scher, H.; Schlesinger, M. F.; Bendler, J. T. *Phys. Today* **1991**, *44*, 26.

(29) Siebrand, W.; Wildman, T. A. *Int. Rev. Phys. Chem.* **1986**, *5*, 251.
(30) Thangaraj, A.; Ganapathy, S. *Indian J. Chem.* **1990**, *29A*, 1080.
(31) Hayashi, S.; Ueda, T.; Hayamitzu, K.; Akiba, E. *J. Phys. Chem.* **1992**, *96*, 10928.
(32) Chudek, J. A.; Hunter, G.; Rochester, C. H.; Smith, T. F. S. *J. Catal.* **1992**, *136*, 246.
(33) Devreux, G. F.; Boilot, J. P.; Chaput, F.; Sapoval, B. *Phys. Rev. Lett.* **1990**, *65*, 643.

Table 4. ^{29}Si Spin–Lattice Relaxation Parameters for Various SiC Samples

			4.7 Tesla			11.7 Tesla		
sample	polytype	peak (ppm)	T' (s)	n	no. of points[a]	T' (s)	n	no. of points[a]
abrasive grade BGW43	6H	−14	4600	0.6	13	5400	0.7	14
		−20	4600	0.9	13	7400	0.7	14
		−24	4400	0.5	13	5400	1.0	14
American Matrix platelets	6H	−14	7900	0.6	12			
		−20	12000	0.6	12			
		−24	9600	0.7	12			
NBS 112b	mixture—mainly 6H		very slow—no reliable numbers					
SiC008 (G. R. Finlay)	6H	−14	1060	1.1	16			
		−20	1670	0.7	15			
		−24	880	1.0	16			
Figure 5 of ref 7[b]	6H	−14	3500	0.8	8			
		−20	4900	0.6	8			
		−24	2200	0.8	8			
SiC002 (G. R. Finlay)	3C	−18	400	0.7	20	340	0.7	16

[a] Number of data points used for the least-squares fit. [b] Magnetic field not specified.

(c) The Transition between Exponential and Stretched Exponential Relaxation. Any mechanism that allows all structurally equivalent nuclei to have equal probability of spin-lattice relaxation should reestablish exponential relaxation. Spin diffusion is the most common such mechanism. For magnetically dilute nuclei, inefficient or negligible spin diffusion can be enhanced by isotopic enrichment, which decreases the average separation between nuclei. Thus, isotopic enrichment of ^{29}Si can lead to exponential relaxation in silicates.[34] Similarly, isotopic enrichment of ^{13}C increases the efficiency of spin diffusion, as inferred by the shift of n from 0.5 to intermediate values at 90% enrichment at a single site.[35] Intermediate values of n are also found for ^{29}Si, ^{13}C, and the dilute ^{1}H present in cured hydridopolysilazane-derived ceramic fibers.[36] Also, in organic solids the effects of nearby protons can promote ^{13}C spin diffusion.[37]

Any other factor that provides a mechanism for all nuclei of a given environment to relax equally should also reestablish exponential relaxation. For example mobile, apparently "liquid-like" organic molecules in the pores of zeolites lead to exponential ^{29}Si relaxation,[38] whereas a zeolite with its pores unoccupied undergoes stretched exponential relaxation.[30] In semiconductors, mobile electrons in the conduction band and mobile holes in the valence band should have similar effects.

(d) Exponential Relaxation in High-Purity Silicon Carbide. The occurrence of exponential relaxation in high-purity doped and undoped 6H silicon carbide cannot be attributed to spin diffusion or to motion of atoms or molecules but is fully consistent with the semiconductor nature of silicon carbide.[3,4]

Cubic (3C) silicon carbide has the same structure as diamond and elemental silicon and is a high-band-gap semiconductor, with electrical properties intermediate between those of diamond and silicon. For example its band gap is 2.3 eV compared to 1.1 eV for silicon and 5.5 eV for diamond. Layer stacking has a major effect on silicon carbide semiconductor properties, as evidenced by the difference in band gap between cubic (3C) and 6H silicon carbide: 2.3 vs 3.0 eV.[4]

Dopants such as aluminum, boron, and nitrogen can enter the silicon or carbon sites in the silicon carbide lattice. These group III or V atoms are themselves fixed in position but the holes or unpaired electrons, which they introduce when they replace group IV silicon or carbon atoms, are mobile at ambient temperature.[39] This mobility of unpaired electrons in the conduction band and/or holes in the valence band should reestablish exponential relaxation by giving all atoms of a given silicon or carbon site an equivalent probability of relaxation.

Spin–lattice relaxation in simple semiconductors, especially elemental silicon, was studied in the early days of NMR and found to be dependent on the concentration of free electrons or holes, with conduction band electrons being an order of magnitude more effective than holes in the valence band.[40] Also, spin–lattice relaxation is independent of magnetic field in semiconductors.[15] All of this is consistent with our work on high-purity 6H silicon carbide: aluminum doping (providing holes) is much less effective than nitrogen doping (providing free electrons) in the same concentration range, and there is no magnetic field dependence (Tables 1 and 2). Holes are much less mobile than free electrons in all of the silicon-like four-coordinate semiconductors.[4] Greater mobility apparently corresponds to perturbing a larger proportion of nuclei in a given time period, and hence more effective relaxation.

As discused earlier, stretched exponential relaxation occurs when **fixed** paramagnetic impurities are predominant. In silicon carbide these are likely to be paramagnetic transition metal atoms. Vanadium and titanium, in particular, are known to be common impurities in Lely process single crystals of silicon carbide; vanadium can occupy the various silicon sites in the lattice.[41] Just as with Fe^{2+} or Fe^{3+} in silicate minerals,[17,18] the unpaired electrons should stay localized on these atoms, which are electrically active deep level defects.[41] As fixed paramagnetic centers become few, mobile conduction band and valence band electrons should provide the predominant mechanism of relaxation, and stretched exponential should merge into exponential relaxation, i.e., the exponent n should increase. This is consistent with our work. Intermediate values of n are consistent with contributions to relaxation from both localized and mobile unpaired electrons, or possibly to partial mobility of the unpaired electrons.

Even with no impurities at all, an intrinsic semiconductor would have some level of occupation of the conduction band by thermal excitation of electrons from the valence band,[39] and these would be effective at relaxing nuclei. But since 6H silicon carbide is a high-band-gap semiconductor this effect should be negligible at ambient temperature and probably does not contribute

(34) Kirkpatrick, R. J.; Howell, D.; Phillips, B. L.; Cong, X.-D.; Ito, I.; Navrotsky, A. *Am. Mineral.* **1991**, *76*, 673.
(35) Maiti, B.; McGarvey, B. R. *J. Magn. Reson.* **1984**, *58*, 37. Also see: McGarvey, B. R. *J. Magn. Reson.* **1989**, *82*, 253.
(36) Lewis, R. H.; Wind, R. A.; Maciel, G. E. *J. Mater. Res.* **1993**, *8*, 649.
(37) Tycko, R.; Dabbagh, G. *Isr. J. Chem.* **1992**, *32*, 179 and references therein.
(38) Challoner, R.; Harris, R. K.; Packer, K. J.; Taylor, M. J. *Zeolites* **1990**, *10*, 539.
(39) (a) Cheetham, A. K.; Day, P. *Solid State Chemistry: Techniques*; Clarendon Press: Oxford, 1987; Chapter 8. (b) Borg, R. J.; Dienes, G. J. *The Physical Chemistry of Solids*; Academic Press: Boston, 1991; Chapter 7. (c) Wold, A.; Dwight, K. *Solid State Chemistry. Synthesis, Structure, and Properties of Selected Oxides and Sulfides*; Chapman and Hall: New York, 1993; Chapter 3, and references therein.
(40) Shulman, R. G.; Wyluda, B. J. *Phys. Rev.* **1956**, *103*, 1127.
(41) Schneider, J.; Maier, K. *Physica B, Condensed Matter* **1993**, *185*, 199 and references therein.

significantly to relaxation, even in our "undoped" sample. Trace amounts of impurities are likely to be more important.

A similar changeover occurs in the nature of ^{13}C spin–lattice relaxation in diamond, an extremely high bandgap semiconductor. Industrial diamond powder (impure)[42] and chemical vapor deposited diamond film[43] undergo fairly efficient stretched-exponential relaxation ($n = 0.5$) whereas a boron-doped semiconducting diamond crystal undergoes exponential relaxation (but very slowly).[44]

(e) Nitrogen Doping: Differences in Relaxation among Sites. Only silicon carbide among the silicon-like four-coordinate semiconductors has polytypes like 6H, and hence has NMR-distinguishable sites for the same nucleus that differ only in their next-nearest and further neighbor environments. Hence silicon carbide provides a unique opportunity to approach four-coordinate semiconductors via the local-site way of thinking that NMR fosters.

Spin–lattice relaxation in nitrogen-doped 6H silicon carbide is unique in being highly site-dependent. Not only do carbon sites relax much more rapidly than the corresponding silicon sites, but also there are unprecedented differences in relaxation efficiency among the different carbon, and among the different silicon, sites: a factor of 20 for ^{13}C, and a factor of 4 for ^{29}Si. This gives a factor of 80 overall, between the slowest relaxing ^{29}Si and the fastest relaxing ^{13}C site, among sites that are very similar crystallographically. For both nuclei, the type C site (the highest-frequency ^{13}C peak and the center ^{29}Si peak, assigned on the basis of its much larger chemical shift anisotropy[9]) is the slowest relaxing.

It is the fast-relaxing type A and type B carbon sites that are truly anomalous: these carbon sites in our highest-concentration nitrogen-doped sample (1.45×10^{18} nitrogen atoms/cm^3, i.e., 2.4 mM) provide the smallest T_1 values that we have determined in any silicon carbide sample.

Differences in relaxation efficiency should be related to differences in unpaired electron density at the different sites, and hence should provide insight into site-specific properties of the conduction band. Interestingly, the slow-relaxing ^{13}C site relaxes about as efficiently as the two fast-relaxing ^{29}Si sites. Also, the type A and type B sites always have the same T_1 value, within experimental error, in any given sample in the ^{13}C spectrum, and also in the ^{29}Si spectrum.

Valence band electrons are certainly more strongly attracted to the more electronegative carbons than they are to the silicons. If the unpaired electrons from the nitrogen atoms that have entered the conduction band behave similarly, it seems reasonable that carbon relaxation should be more efficient than silicon relaxation, due to the greater unpaired electron density near the carbon sites. But this simplistic approach does not account for differences among the carbon, or among the silicon, sites.

The electronic environments about the different carbon (and silicon) sites must differ considerably. It has already been recognized that nitrogen donors in the three different carbon sites have very different properties. As determined by ESR, the unpaired electron spin density at nitrogen donors in the hexagonal (h) carbon site is only about one-tenth of that occurring at nitrogen donors in the two quasicubic sites in 6H SiC.[41] Assuming that the electronic environments at the carbon sites are similar whether the sites are occupied by carbons or by nitrogens, differences such as these would account for the great differences in ^{13}C spin–lattice relaxation behavior. The much higher unpaired electron density in the conduction band at the type A and type B sites accounts for their more efficient ^{13}C spin–lattice relaxation. The differences in peak widths of the ^{13}C signals (60 Hz for the type A and type B sites, but only 36 Hz for the slow-relaxing type C site, at 11.7 T; see Figure 2) are consistent with broadening due to high unpaired electron density at the type A and type B sites. There are no pronounced differences in peak widths among the corresponding ^{29}Si signals (all about 25 Hz), consistent with lack of any similar amount of excess unpaired electron density about any silicon site.

Charge density effects in silicon carbide have been calculated by Qteish, Heine, and Needs[45] and used to rationalize the number of ^{29}Si and ^{13}C NMR peaks and the range of chemical shifts observed in silicon carbide polytypes. They find that the intrinsic dipole moments in any silicon carbide polytype except 3C lead to substantial electric fields, and these lead to variations in electrical potential at the different sites. They propose that mobile carriers would be sufficiently localized to take advantage of the differences in potential at different sites, and hence would tend to occupy the sites of lowest potential. Our spin–lattice relaxation work, indicating very different unpaired electron densities at different sites, supports their proposal.

It is noteworthy that no such discrimination among sites has been detected in the aluminum-doped (p-doped) material. While the total concentration of aluminum in our aluminum-doped sample has been well-established, it is likely that only a fraction of the aluminum is activated.[46] Some may not be in lattice sites, and what is in the lattice is not necessarily all ionized to provide carriers. Thus there may be far fewer holes in the valence band than calculated from the total aluminum concentration. Alternatively, if essentially all of the aluminum is incorporated in the lattice and all sites are ionized, then the holes are unselective (as well as not very effective) in relaxing the different sites.

(f) Lower-Purity Samples. The sample of Table 3, undergoing stretched exponential relaxation with an intermediate n value of 0.7, occupies an intermediate position between the semiconductor grade and the low-purity 6H silicon carbide samples. There is negligible change in appearance of the spectrum with the τ value, indicating that there are no local regions that relax differently from the bulk material, consistent with the homogeneous appearance of its electron back scattering image. Randomly distributed fixed paramagnetic impurities may be competing with mobile electrons in causing spin–lattice relaxation in this sample.

Spectra of the lower-purity samples of Table 4 vary widely in resolution and relaxation behavior but all appear to be heterogeneous to some extent, with fast-relaxing components near paramagnetic centers giving broadened signals. Although there are large uncertainties in their T' and n values, the n values tend to be closer to 0.5 than to 1. There is one exception, sample SiC008, which also has less efficient relaxation (by a factor approaching 2) for the center peak, which would be consistent with the presence of some mobile valence band electrons resulting from nitrogen doping.

Some uncertainty in T' and n is inherent in the nature of the samples. It is difficult to define relaxation behavior in a unique manner for heterogeneous samples in which different local regions with different relaxation characteristics contribute to the same NMR peak. Nevertheless, use of the stretched exponential function, with time constant T' and variable n, does give a simple **empirical** description of relaxation behavior in such systems.

Mooney[7] proposed the presence of a rapidly-relaxing material as well as a slow-relaxing material in his silicon carbide samples. The ^{29}Si relaxation behavior shown in his Figure 5 does however fit a single stretched exponential function with intermediate n values (our Table 4). His proposal is correct in the sense that stretched exponential relaxation arises from samples which inherently have fast-relaxing and very-slow-relaxing components;

(42) Henrichs, P. M.; Cofield, M. L.; Young, R. H.; Hewitt, J. M. *J. Magn. Reson.* **1984**, *58*, 85.
(43) Lock, H.; Maciel, G. E.; Johnson, C. E. *J. Mater. Res.* **1992**, *7*, 2791.
(44) Hoch, M. J. R.; Reynhardt, E. C. *Phys. Rev. B: Condensed Matter* **1988**, *37*, 9222.
(45) Qteish, A.; Heine, V.; Needs, R. J. *Physica B. Condensed Matter* **1993**, *185*, 366.
(46) Parrish, M. A., Cree Research, Inc., Durham, NC, private communication.

however they are not discrete components but the limiting cases in a continuum which is described by the stretched exponential expression.

Perhaps surprisingly, crude abrasive grade samples such as BGW43 need not relax more efficiently than the semiconductor grade samples. In fact, apart from a small signal component that does relax efficiently and is selectively detected under commonly-used 5 s or even 5 min pulse repetition rates and can often be selectively depleted by acid washing,[6,47] some of these relax very inefficiently indeed. This may mean fairly high purity within crystals, and the presence of surface and/or additional crystalline material which is much less pure. There certainly are further, non-SiC phases containing the bulk of the impurities in the National Bureau of Standards sample 112b that might affect relaxation in nearby silicon carbide local regions.

Yet slow relaxation need not correspond to high purity. There are numerous types of impurities and defects that need not involve paramagnetic centers, such as mixtures of polytypes within a crystal, stacking faults, and antisite defects. Moreover, the lifetime of the electron spin states (the electron T_1) plays a crucial role in the effectiveness of the unpaired electron in relaxing nuclei. Silicon carbide is truly a complex system, with many possible types of impurities,[1] and much remains to be learned. Interference among different kinds of impurities, that might themselves be effective in spin–lattice relaxation, could make relaxation less efficient. Thus mobile electrons of the conduction band might fall into the deep level impurity sites and become immobilized, localizing their effects and causing reversion to stretched exponential relaxation.

Conclusions

Silicon carbide spin–lattice relaxation efficiency can vary by orders of magnitude, depending on impurities. There are surprisingly large differences in relaxation efficiency at different sites in nitrogen-doped 6H silicon carbide, apparently arising from greatly differing conduction band unpaired electron densities, and these provide insight into the semiconductor behavior of 6H silicon carbide. It would be intriguing to extend this work to other polytypes. The importance of conduction band mobile electrons in spin–lattice relaxation need not be limited to silicon-like species since many systems both simple and complex show semiconductor behavior to varying degrees.[48]

Although the drawbacks of inefficient spin–lattice relaxation can be severe, it is still possible to extract useful information. The interplay of different relaxation mechanisms (exponential vs stretched exponential) can provide valuable insight into the relaxation processes and the nature of the impurities in such materials, in which mobile and localized paramagnetics compete in relaxing the nuclei, but careful measurement and curve fitting are required to obtain meaningful values of the exponent n. While the underlying principles of stretched exponential spin–lattice relaxation have been derived decades ago,[27] and its occurrence seems to be widespread in dilute spin-$^1/_2$ nuclei in solids, this phenomenon has been neglected in the rapidly growing field of MAS NMR of inorganic materials and minerals.

Many new synthetic-material environments, including surfaces and films as well as bulk materials, are being studied by NMR, but there are pitfalls as well as advantages in applying NMR to materials that can be inhomogeneous and/or can have widely varying impurities. The present study of spin–lattice relaxation in a particularly favorable model system, the 6H polytype of silicon carbide, illustrates the variety of relaxation behavior that can be observed in different samples of a superficially-simple compound. Relaxation measurements in the rotating frame may provide further information. There is widespread current interest in both the semiconducting and the high-tech ceramic aspects of silicon carbide, that merits extension of this work.

Acknowledgments. We thank Prof. Mary Frances Richardson (Brock University), Prof. Alex D. Bain (McMaster University), and Prof. Robert F. Davis (North Carolina State University) for helpful discussions, Mr. Tim Jones, Mr. James Shoemaker (Brock), Mr. Brian Sayer, and Dr. Don Hughes (McMaster) for assistance with the instrumentation, and the Natural Sciences and Engineering Research Council of Canada for financial support. We also thank Prof. Robert F. Davis, American Matrix, Inc., Knoxville, TN, and General Abrasive, Niagara Falls, Ontario, for providing silicon carbide samples and Prof. N. M. Halden, University of Manitoba, for providing electron microprobe analyses.

(47) Hartman, J. S.; Shoemaker, J. A. W. Unpublished work.

(48) Moran, K. L.; Gier, T. E.; Harrison, W. T. A.; Stucky, G. D.; Eckert, H.; Eichele, K.; Wasylishen, R. E. *J. Am. Chem. Soc.* **1993**, *115*, 10553.